

# Microscale Templating of Materials across Electrospray Deposition Regimes

Michael J. Grzenda <sup>1</sup>, Maria Atzampou <sup>2</sup>, Alfusainey Samateh <sup>3</sup>, Andrei Jitianu <sup>3,4</sup>, Jeffrey D. Zahn <sup>2</sup> and Jonathan P. Singer <sup>1,5,\*</sup>

<sup>1</sup> Department of Materials Science and Engineering, Rutgers University, Piscataway, NJ 08854, USA

<sup>2</sup> Department of Biomedical Engineering, Rutgers University, Piscataway, NJ 08854, USA

<sup>3</sup> Department of Chemistry, Lehman College, of the City University of New York, New York 10468, NY, USA

<sup>4</sup> Ph.D. Program in Chemistry and Biochemistry, The Graduate Center of the City University of New York, 365 Fifth Avenue, New York, NY 10016, USA

<sup>5</sup> Department of Mechanical and Aerospace Engineering, Rutgers University, Piscataway, NJ 08854, USA

\* Correspondence: jonathan.singer@rutgers.edu

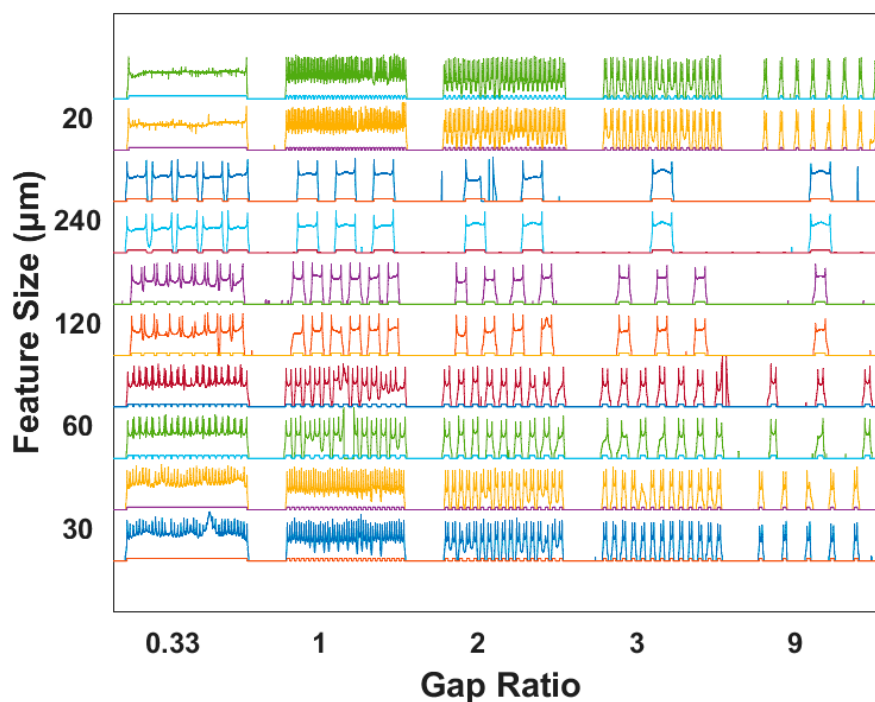


**Figure S1.** All aligned profilometry data for the test pattern sprayed with 30 °C Polystyrene .

**Citation:** Grzenda, M.J.; Atzampou, M.; Samateh, A.; Jitianu, A.; Zahn, J.D.; Singer, J.P. Microscale Templating of Materials across Electrospray Deposition Regimes. *Coatings* **2023**, *13*, 599. <https://doi.org/10.3390/coatings13030599>

Academic Editor: Rainer Hippler

Received: 10 February 2023

Revised: 3 March 2023

Accepted: 6 March 2023

Published: 11 March 2023



**Copyright:** © 2023 by the authors. Submitted for possible open access publication under the terms and conditions of the Creative Commons Attribution (CC BY) license (<https://creativecommons.org/licenses/by/4.0/>).

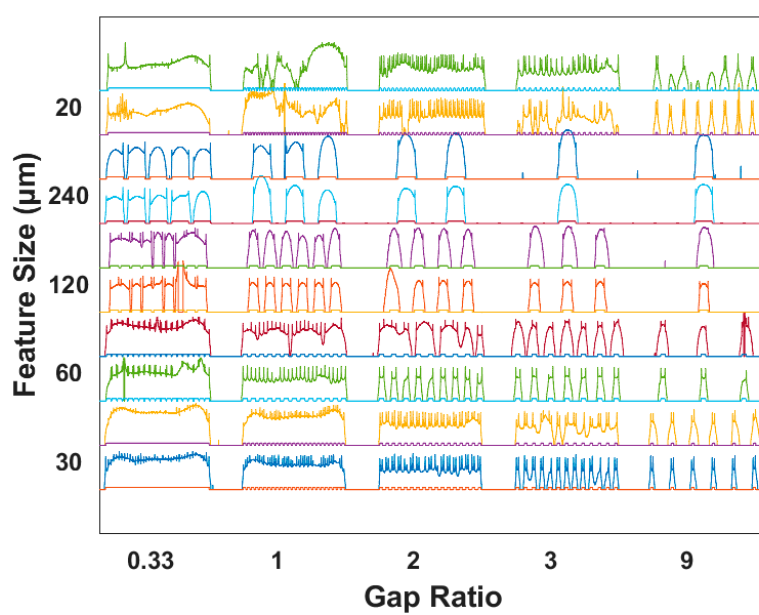


Figure S2. All aligned profilometry data for the 100 °C Polystyrene sample.

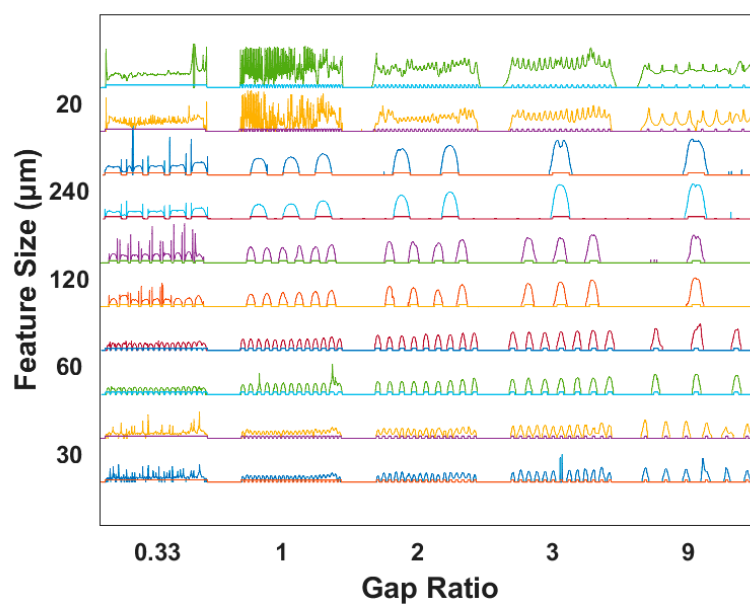


Figure S3. All aligned profilometry data for the melting gel sample.

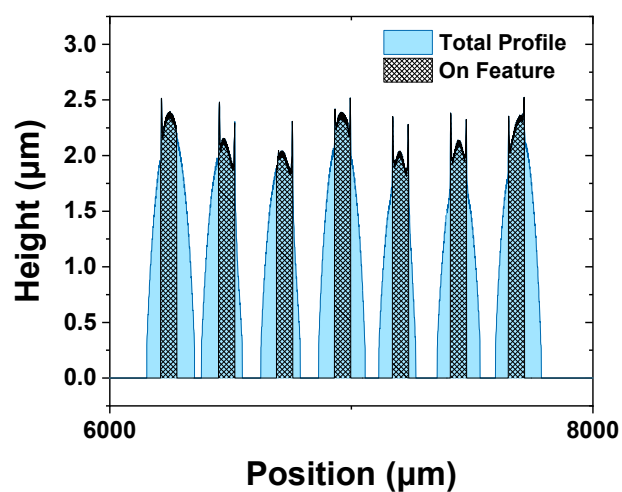
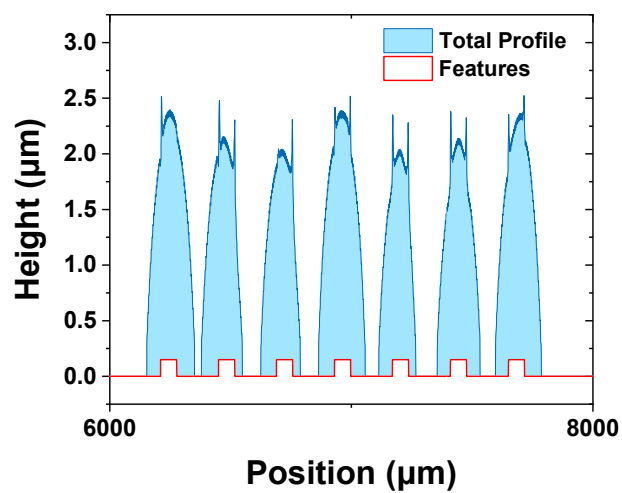
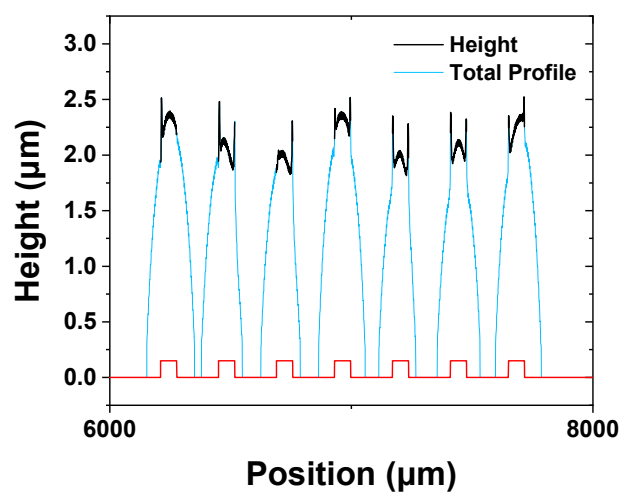


Figure S4. Visual representation of (top)  $H_g$ , (middle)  $\rho_g$ , and (bottom)  $\sigma_g$ .

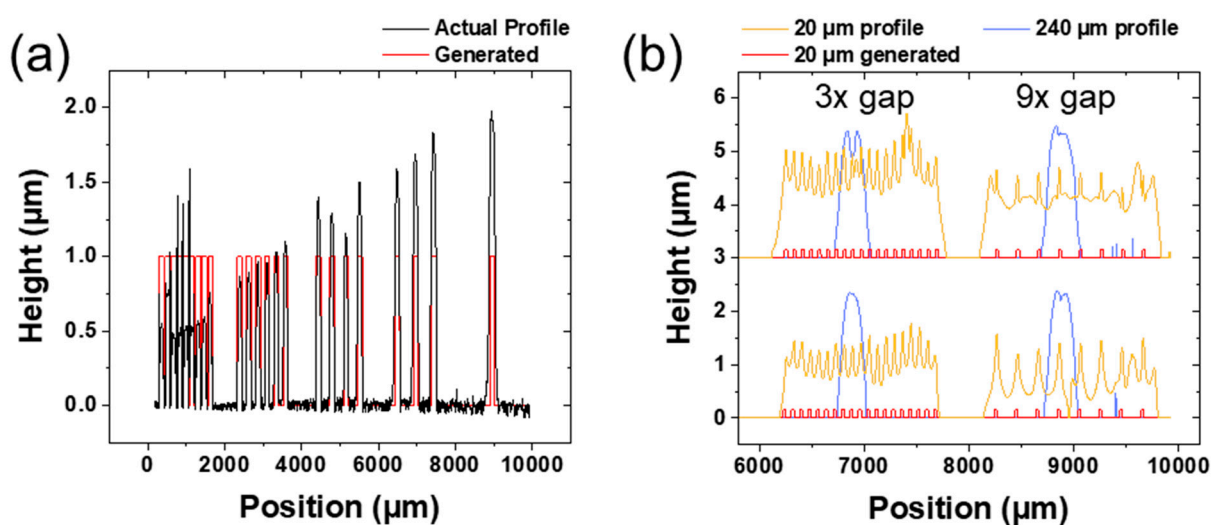


Figure S5. Profile scan of (a) the 120 μm feature of the MG test pattern and (b) the 20 μm features overlaid with the 240 μm features. (Left) 3× gap and (Right) 9× gap.

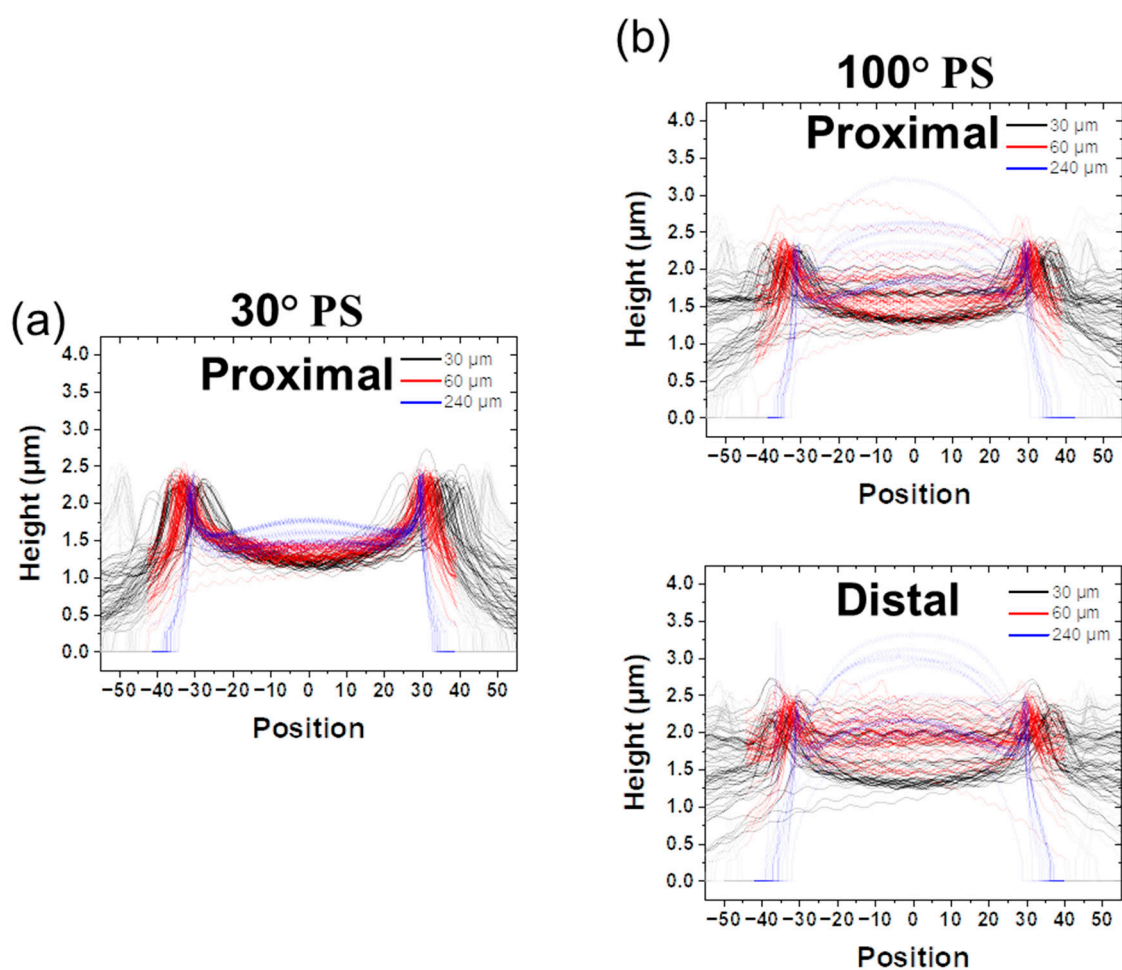


Figure S6. Overlays of the 30, 60, and 240 μm feature profiles, standardized by width for (a) PS 30 °C Proximal and (b) PS 100 °C Proximal and Distal. Adjoining features have been colored light gray when present.

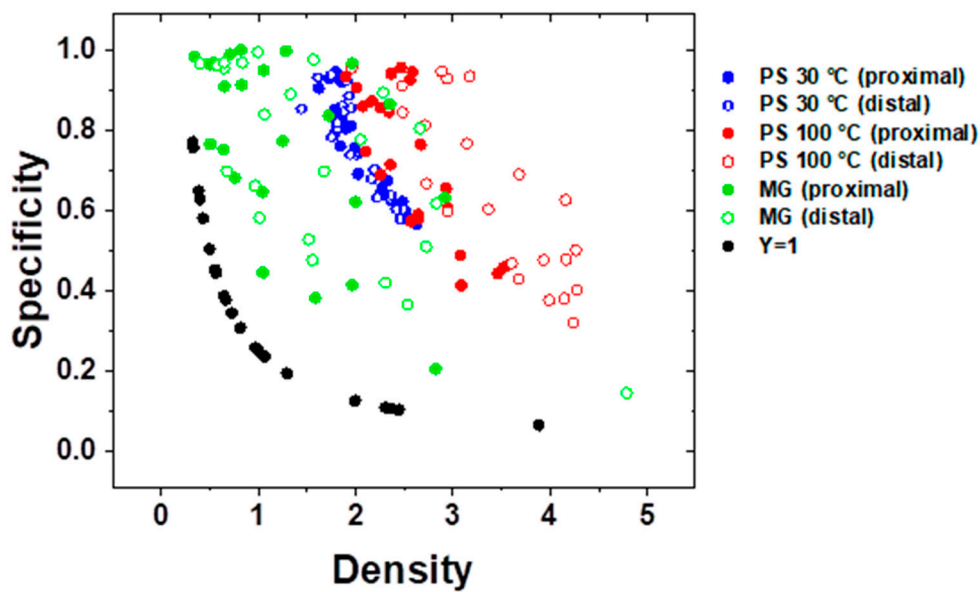


Figure S7. Specificity versus density for all data sets.

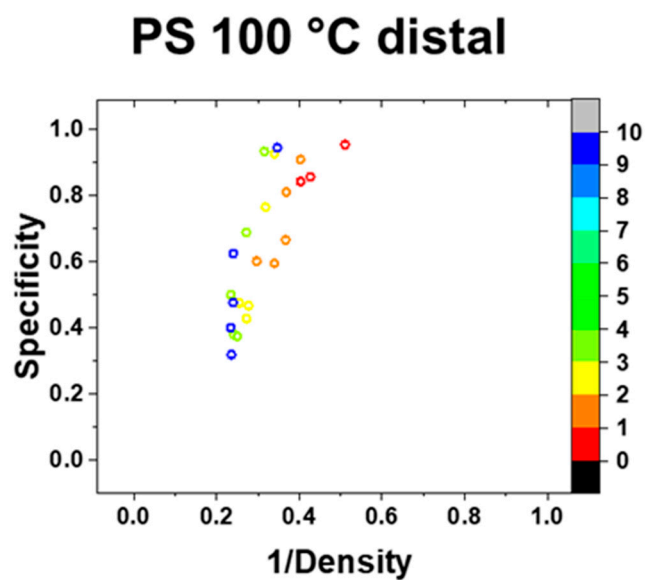


Figure S8. Specificity vs 1/Density with color maps denoting gap ratio for PS 100 °C distal-only.

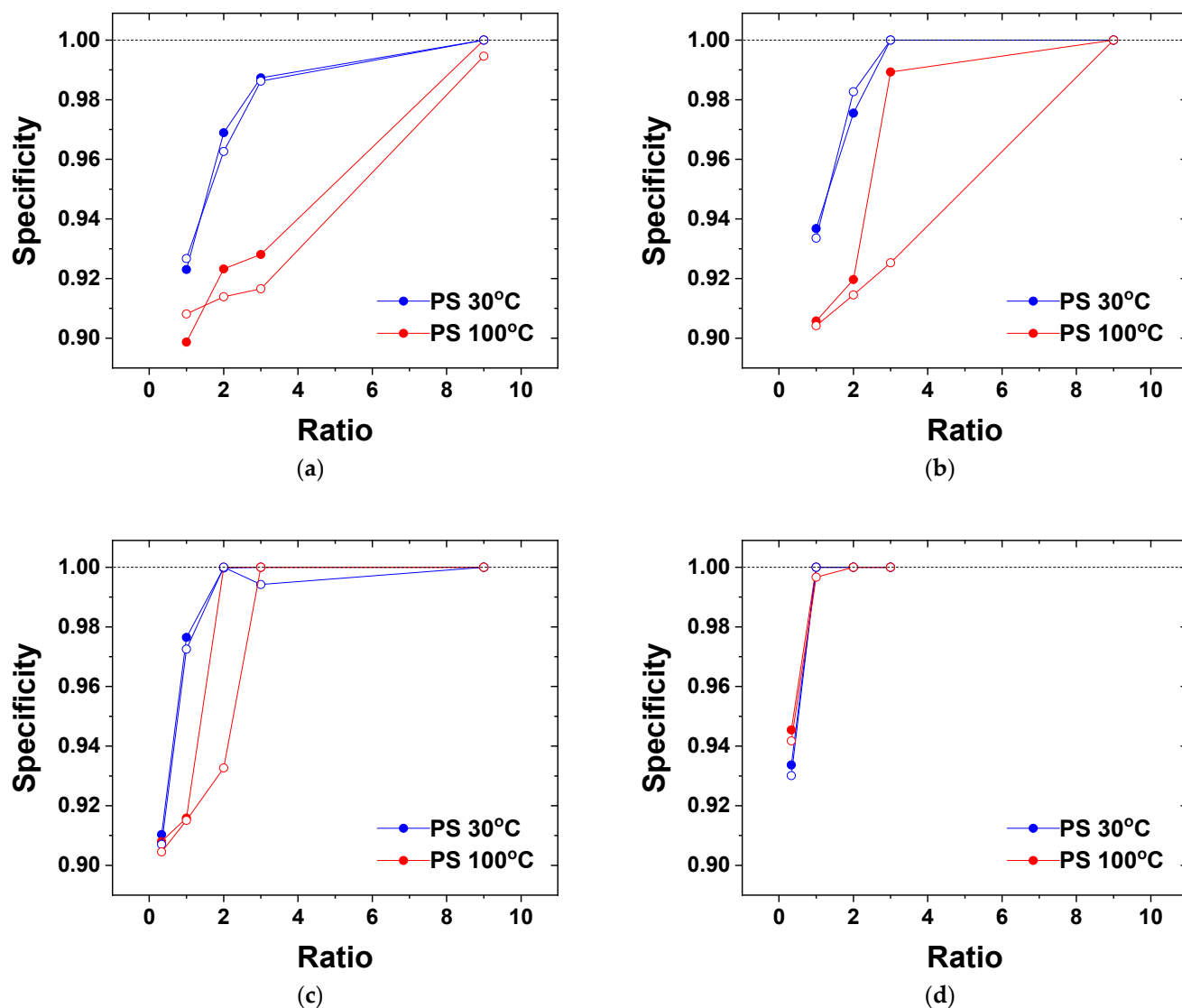
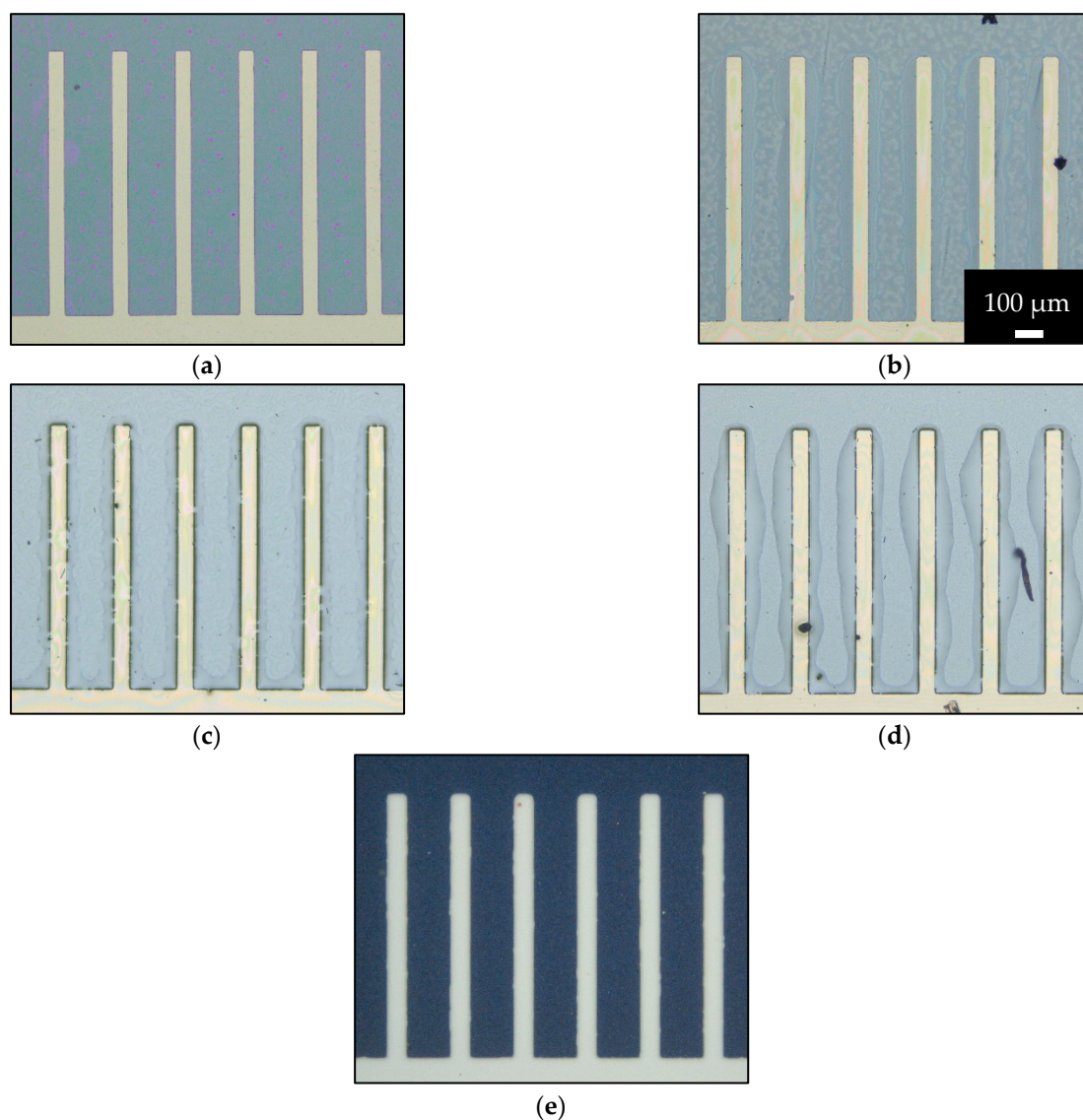


Figure S9. Expanded gap specificity by feature size. (a) 20  $\mu\text{m}$ , (b) 30  $\mu\text{m}$ , (c) 60  $\mu\text{m}$  and (d) 120  $\mu\text{m}$ .



**Figure S10.** Microscope images of the 60  $\mu\text{m}$  feature/3 $\times$  gap for (a) blank test pattern, (b) MG, (c) PS 30  $^{\circ}\text{C}$ , and (d) PS 100  $^{\circ}\text{C}$ , and (e) methylcellulose. Methylcellulose is also a self-limiting material, here shown for generalizability. This pattern was sprayed for 2 h under similar conditions to the other materials. However, it was not densified, making it easier to image with darkfield.



**Simulation Details:** The simulation was conducted in COMSOL Multiphysics® (version 6.0, 2022, COMSOL Inc, Burlington, MA, USA) with a 3D cylindrical domain with 50 cm radius and height. All surfaces of the domain were zero charge. A grounded boundary was placed on the top surface of a 0.5 mm thick, 2 in radius “wafer” 6 cm above which a 1 in “needle” with a 0.25 mm diameter was placed at 6 kV of potential. The interiors of these domains were not simulated. A virtual cylinder was placed at the center of the wafer domain to assist with mesh structuring. These features can be most clearly seen in (a) and (b). A mask plane was placed 10  $\mu\text{m}$  above the wafer surface (c) and simulated as a charged surface representing the Parylene coating. Since the magnitude of this charge is unknown, it was parametrized at a constant value, which is a major simplification of this simulation since the accumulated charge on the insulating surface need not be uniform. To simulate the electrode pattern, regions of this surface were left uncharged. For this simulation, we chose a 120  $\mu\text{m}$  feature with a spacing corresponding to 3 times the feature size. To determine effects of distal and proximate positioning, a 500  $\mu\text{m}$  pad was located both at the base and 500  $\mu\text{m}$  from the end of the features. Results from the simulation are shown in (d). The top row depicts a single feature sliced along the  $y = 0$  plane. As the surface charge increases, the field lines transition from denser at the edges with peaks slightly inside the feature to fully focused to the center. The bottom row depicts a single feature sliced along the  $x = 0$  plane. The domains are outlined in red, with guides to the eye (from left to right, also shown in (c)) for the start (labeled ‘i’) and end of the pad at the base of the feature, the end of the feature, and the start and end (labeled ‘ii’) of the pad placed above the feature. As the field increases, there is increased density of field lines near the end of the feature and decreased field lines near where the pad begins at its base.

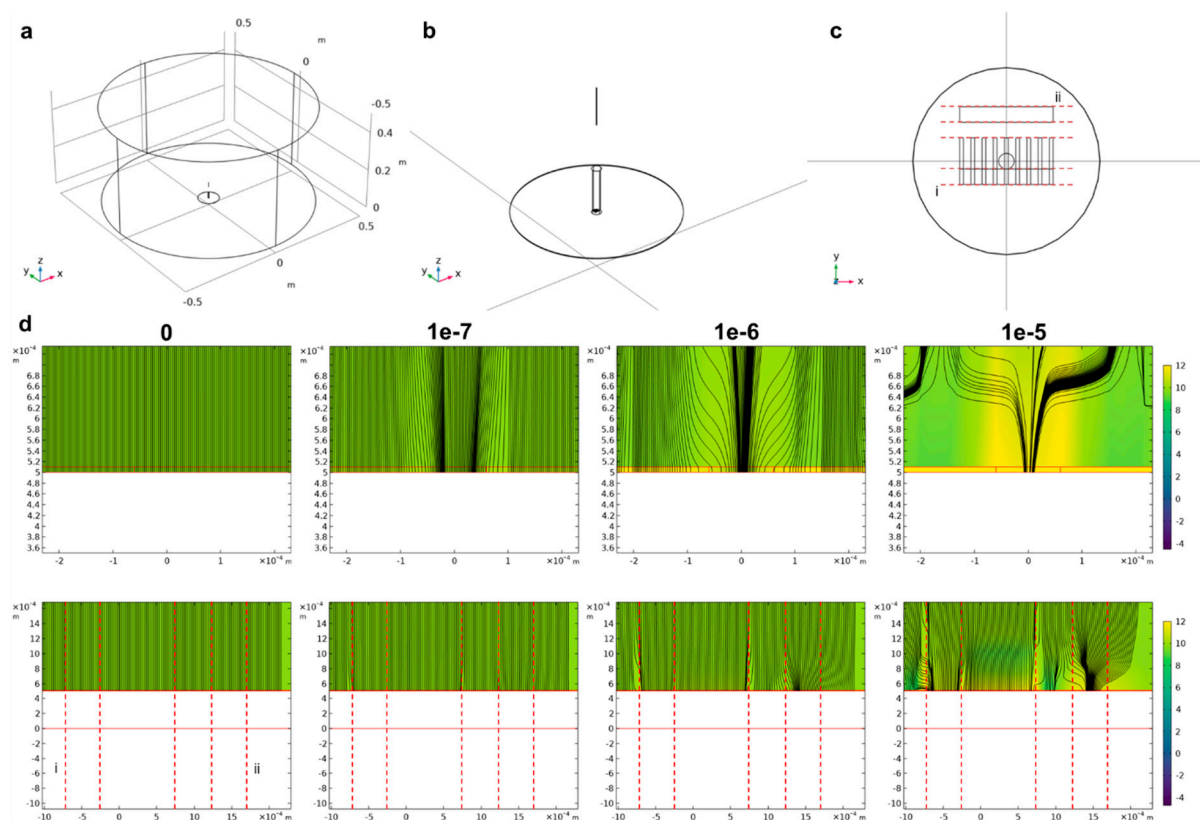


**Figure S11.** (a–c) Pictures of the simulation cell for the electrostatic spray simulation. (d) 2D slices of the simulation with color maps representing a log scale of the electric field magnitude and electric field lines (first order analogs for the spray path). The domains are outlined in red. Due to the strong field in between the charged and grounded surface, the color map was set to saturate at  $1\text{e}12$ . The charge on the charged surface is listed above each column in units of  $\text{C}/\text{m}^2$ .